THE JOURNAL OF PHYSICAL CHEMISTRY B

Article

pubs.acs.org/JPCB

# Molecular Dynamics and Umbrella Sampling Study of Stabilizing Factors in Cyclic Peptide-Based Nanotubes

R. Vijayaraj,[†,‡] S. Van Damme,[‡] P. Bultinck,[‡] and V. Subramanian*[,†]

[†]Chemical Laboratory, CSIR-Central Leather Research Institute, Adyar, Chennai 600 020, India

[‡]Department of Inorganic and Physical Chemistry, Ghent University, Krijgslaan 281(S3), Gent 9000, Belgium

Supporting Information

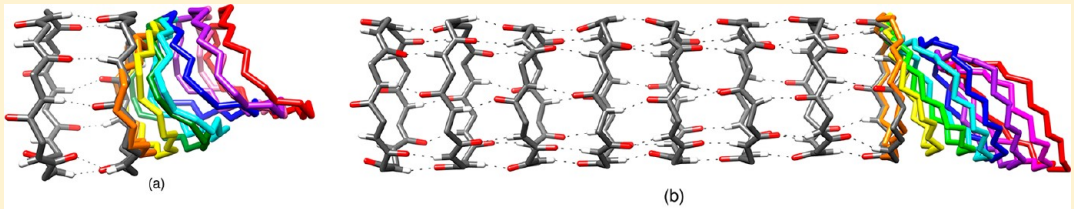


Dissociation mechanism of self-assembled CPs in different solvent environments

**ABSTRACT:** In this study, the dissociation mechanism of self-assembled cyclic peptides (CPs) has been investigated using classical/steered molecular dynamics simulations combined with umbrella sampling techniques in a polar and a nonpolar solvent. The stability of cyclic peptide nanotubes (CPNTs) with different surface polarity, {*cyclo*-[(D-Trp-L-Leu)$_4$]}$_8$ and {*cyclo*-[(L-Gln-D-Ala-L-Glu-D-Ala)$_2$]}$_8$, are explored in detail. It is observed from the results that the CPNTs are less dynamic in the nonpolar solvent than in the polar solvent. The dissociation of CPs from a lower oligomeric form is achieved by gradual breaking of interactions, requiring relatively little force. In higher oligomeric CPNTs, the dissociation takes place by collective breaking of interactions with significantly higher force. During the dissociation process, the tendency for collective breaking of various intermolecular interactions increases from the terminal to the core of the CPNT. The breaking of backbone−backbone hydrogen bonding is the critical point in the dissociation of CPs which is followed by the annihilation of various side chain−side chain interactions. The polarity of the solvent plays a decisive role in the dissociation mechanism of self-assembled CPs. It is evident from the calculated free energy of binding values that the overall stability of CPNT is higher in the nonpolar solvent than in the polar solvent.

## INTRODUCTION

During the past two decades, various experimental and theoretical studies have been carried out on the structure and stability of cyclic peptide nanotubes (CPNTs) owing to their potential applications in the field of active transportation of ions and drug molecules through the lipid bilayer.[1−16] It is found from previous studies that cyclic peptides (CPs) consisting of alternate L/D amino acids can self-assemble into extended hollow tubular structures by forming antiparallel $\beta$-sheet-like hydrogen bonding (H-bonding) between the backbones of successive CP units.[17−26] In addition to the backbone−backbone H-bonds, the self-assembled CPs are further stabilized by the side chain−side chain interactions between subsequent CP units. In the self-assembly of CPs, the antiparallel stacking is dominant over the parallel stacking because of the higher interaction energy in the antiparallel stacking.[20,27−32] The arrangement of alternate L/D amino acids imposes the side chains to orient toward the surface of the tube. The lumen of the tube is free from amino acid side chains, and it provides the characteristic transport application for CPNTs.[4,9,11,15,29,33−35] The feasibility to modify the diameter of the CPNT by selecting an appropriate number of amino acids in the CPs enhances the transport of molecules with different sizes.[12,27,36]

In the self-assembly of CPs built from the standard amino acids including D isomers, the hollow tubular structure is less affected, regardless of the presence of various amino acids, because of the systematic backbone−backbone H-bonds. However, the stability of CPNT is modulated by the presence of various amino acids and their side chain−side chain interactions. Recently, a density functional theory-based study on CPNT has revealed that the cooperativity in the interaction energy of self-assembled CPs is attained by the side chain−side chain interactions rather than the backbone−backbone H-bonds.[32,37] Even though the backbone H-bonds lack cooperativity in the interaction energy, they are less affected by the polar solvent medium and play a vital role in the stability of self-assembled CPs. When designing the CPNTs, the nature of the tube surface (electrophilic/hydrophilic) can be tailored by selecting appropriate amino acids. In general, the surface property is opted to be complementary to the bulk medium.

**Received:** April 10, 2012
**Revised:** July 13, 2012
**Published:** July 17, 2012

**Scheme 1. Schematic Representation of Various Groups Being Pulled from the Self-Assembly[a]**

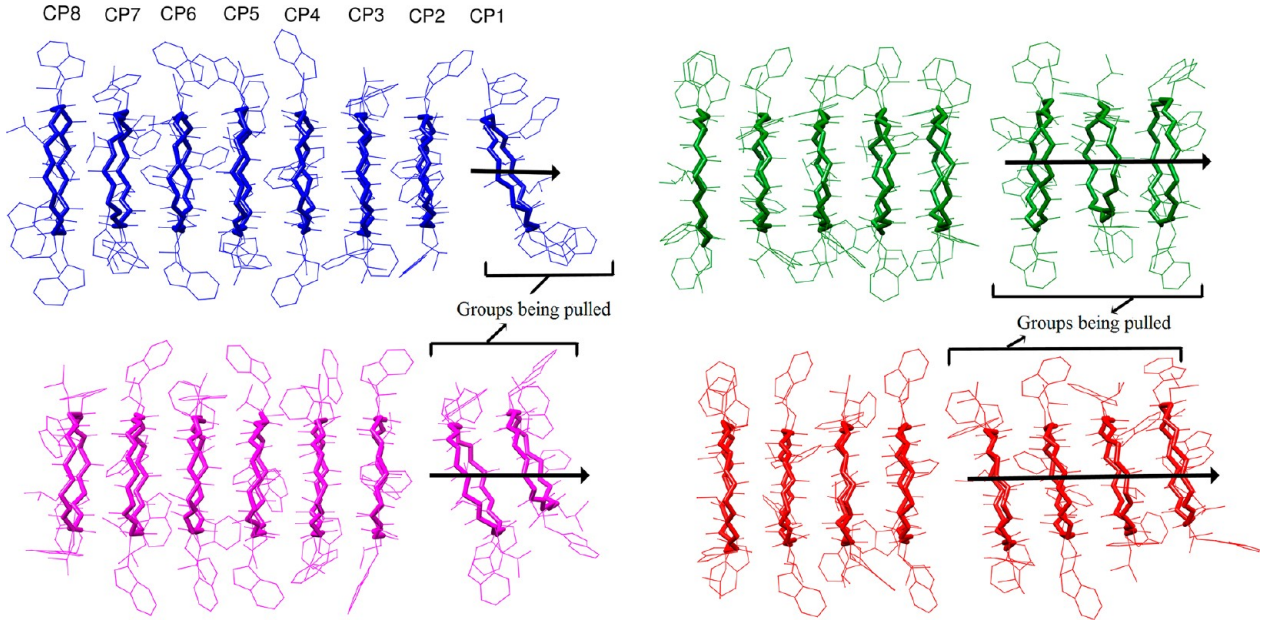


[a]The pulling direction is represented by an arrow.

For instance, a CPNT can be tailored to have a nonpolar surface in order to diffuse into the lipid bilayer.[15,28] Nevertheless, self-assembly happens before the lipid bilayer diffusion;[15,28] hence, it is crucial to understand the stability of CPNTs in both polar and nonpolar environments.

In a previous study, we investigated the critical steps involved in the self-assembly of CPs using $\{cyclo[(\text{D-Ala-L-Ala})_4]\}_n$, (where $n$ represents the number of CPs, which ranges from 1 to 8) as model systems using classical molecular dynamics (MD) simulation.[38] In the present study, the interaction between CPs has been investigated using classical, steered MD combined with the umbrella sampling (US) technique in polar and nonpolar solvent mediums for $cyclo[(\text{D-Trp-L-Leu})_4]$ and $cyclo[(\text{L-Gln-D-Ala-L-Glu-D-Ala})_2]$ as model systems. It is found from preliminary binding energy calculations on various CPNTs ($cyclo[(\text{D-Ala-L-Phe})_4]$, $cyclo[(\text{D-Ala-L-Leu})_4]$, $cyclo[(\text{D-Ala-L-Gln})_4]$, $cyclo[(\text{L-Gln-D-Ala-L-Glu-D-Ala})_2]$, $cyclo[(\text{D-Gln-L-Leu})_4]$, $cyclo[(\text{D-Trp-L-Leu})_4]$, and $cyclo[(\text{D-Trp-L-Leu})_3\text{-D-Gln-L-Leu}]$) using the MM/PBSA method that $cyclo[(\text{D-Trp-L-Leu})_4]$ leads to the formation of CPNT with high stability. On the other hand, the CPNT formed from $cyclo[(\text{L-Gln-D-Ala-L-Glu-D-Ala})_2]$ has lower stability. Thus, these two CPNTs have been chosen for the present investigation. The following points have been addressed in this investigation: (a) structural stability of CPNTs in polar and nonpolar solvent environments, (b) the dissociation mechanism of CPs from the CPNT, and (c) free energy of formation of CPNT.

## COMPUTATIONAL DETAILS

**Classical Molecular Dynamics.** The $cyclo[(\text{D-Trp-L-Leu})_4]$ peptide was stacked to form both a dimer and an octamer. By dimer, we mean a stack of only 2 CPs; an octamer is a stacked arrangement of 8 CPs. The dimer and octamer are designated as $(WL)_2$ and $(WL)_8$, respectively, using the single letter amino acid code. The $cyclo[(\text{L-Gln-D-Ala-L-Glu-D-Ala})_2]$ peptide was self-assembled into an octamer model system, which is denoted as $(QAEA)_8$. All the systems were constructed by antiparallel stacking of one CP unit with respect to another. The antiparallel stacking ensures the interactions between the homochiral residues of adjacent CP units. The $(WL)_2$ and $(WL)_8$ systems adopt $C_4$ symmetry, and the $(QAEA)_8$ system exhibits $C_2$ symmetry.

The side chain of Glu in the $(QAEA)_8$ system was protonated to avoid the repulsive electrostatic interaction between the negatively charged carboxylate groups. Each model system was solvated with a cubic box of TIP3P water molecules extending 16 Å away from the molecular surface.[39,40] This results in a box of dimensions of typically 54.9 × 54.9 × 54.9, 78.2 × 78.2 × 78.2, and 74.9 × 74.9 × 74.9 Å$^3$ for the $(WL)_2$, $(WL)_8$, and $(QAEA)_8$ systems, respectively. The $(WL)_2$, $(WL)_8$, and $(QAEA)_8$ model systems contains 5316, 15305, and 13521 water molecules, respectively. The structures of the CPNTs simulated in the water environment (polar medium) are represented as $(WL)_2^{aq}$, $(WL)_8^{aq}$, and $(QAEA)_8^{aq}$.

The $(WL)_8$ and $(QAEA)_8$ systems were simulated in a nonpolar solvent medium by taking nonane as the solvent. The force field parameters for nonane was generated using the Antechamber program of AmberTools 1.5 with the general amber force field.[41,42] The partial charges of nonane were calculated by the RESP fitting technique[43−45] based on the optimized structure and electrostatic potential calculated using the B3LYP/6-31G* method in the Gaussian 03 suite of programs.[46−49] A box consisting of 720 nonane molecules was constructed, and it was further subjected to energy minimization, followed by equilibration in the NPT ensemble for 1 ns. After successful equilibration, the nonane box dimensions were 59.6 × 47.7 × 83.5 Å$^3$. This box was used for simulation of CPNTs in the nonpolar medium. The boxes used for $(WL)_8$ and $(QAEA)_8$ systems contain 687 and 623 nonane molecules, respectively. The nomenclatures used for simulation of $(WL)_8$ and $(QAEA)_8$ systems in the above-mentioned nonane boxes (nonpolar medium) are $(WL)_8^{np}$, and $(QAEA)_8^{np}$, respectively. The $(WL)_2$ system was not considered in a nonpolar medium because this model has been studied before by Khurana et al.[56]


dx.doi.org/10.1021/jp303418a | J. Phys. Chem. B 2012, 116, 9922−9933

Various steps used to simulate all the aforementioned systems were (a) all atom energy minimization for 10000 cycles without any position restraints, (b) equilibration of the solvent molecules for 200 ps by restraining the solute atoms through a harmonic force constant of 1000 kJ $nm^{-2}$ in the NVT ensemble, followed by further equilibration in the NPT ensemble in the absence of positional restraints, (c) production MD simulation for 10 ns in the NPT ensemble using a 2 fs time step. From the production run, structural information was collected every 0.2 fs. All the simulations were carried out with periodic boundary conditions. The pressure was controlled at 1 atm using a Parrinello−Rahman barostat. The protein and nonprotein atoms were coupled to separate temperature-coupling baths, and the temperature was maintained at 300 K with a velocity rescaling thermostat. The particle-mesh Ewald summation method was used for calculating the long-range electrostatic interactions.[50] The short-range and long-range nonbonded interactions were truncated at a 1.4 and 12 Å cutoff, respectively. The linear constraint solver algorithm was used to constrain the bonds involving hydrogen atoms.[51] All calculations were carried out using GROMACS 4.5.5[52,53] employing ff99SB[54] force field parameters.

**Steered Molecular Dynamics and Umbrella Sampling.** Understanding the dissociation of two molecules using classical MD simulation is a computationally time-consuming process. Thus, in a steered molecular dynamics (SMD) simulation, an external force is applied to accelerate this process.[55] The SMD simulations have been successfully performed on various systems. Particularly, the same has been used to calculate the free energy of dimer CPs' self-assembly and also to unravel the transport of ions/drug molecules through CPNT.[10,15,56] The most commonly used method for the calculation of the free energy of binding from the SMD simulation is the Jarzynski equality.[57] The other method is the weighted histogram analysis method (WHAM), which was proposed by Kumar and co-workers.[58] The WHAM method has also been used to calculate the free energy of binding.[59−61] Recently, the WHAM method has been effectively applied to calculate the free energy of binding of amyloid $\beta$-peptide, which is similar to the self-assembly of CPs.[62] Thus, the same methodology was selected to calculate the free energy of binding of CPNTs.

The final structure obtained from the classical MD simulation was used for the SMD or center of mass (COM) pulling simulation. The box dimensions were modified to provide sufficient space to accommodate pulling in the $z$ direction. All SMD simulations were carried out in GROMACS 4.5.5[52,53] employing ff99SB[54] force field parameters. The schematic representations of various groups being pulled in the present study are depicted in Scheme 1. The nomenclature used for pulling of various CP units in both polar and nonpolar mediums are $(WL)^{aq}_{2\rightarrow m}$, $(WL)^{aq}_{8\rightarrow m}$, $(WL)^{np}_{8\rightarrow m}$, $(QAEA)^{aq}_{8\rightarrow m}$, and $(QAEA)^{np}_{8\rightarrow m}$, where $m$ represents the number of CP units in the group being pulled. It ranges from 1 to 4 for octamer systems, and for the dimer system, $m = 1$. It can be seen from Scheme 1 that $m = 1$ denotes the pulling of the CP1 unit and $m = 4$ means the pulling of CP1 to CP4 units from the octamer. Before the pulling simulation, each system was equilibrated for 100 ps in NVT and NPT ensembles by performing a MD simulation. Each COM pulling simulation was carried out to move away the selected group from the self-assembled CPs. During this simulation, the position of the CP unit adjacent to the group being pulled was restrained. This restrained CP unit is referred to as the reference group. The COM pulling simulation time for various systems ranges from 500 ps to 2.5 ns, depending on the nature of the interaction and the targeted pulling distance between the reference group and the group being pulled. A harmonic spring constant of 1000 kJ $mol^{-1}$ $nm^{-2}$ and a pulling rate of 0.004 nm/ps were used for all simulations. To understand the relationship between the pulling velocity and the dissociation pathway, the SMD simulations were performed on the $(WL)^{aq}_{8\rightarrow 1}$ system with different pulling velocities of 0.001, 0.004, and 0.005 nm/ps. The plot of the pulling force vs. time and the dissociation pathway for various pulling velocities are given in Figures S1 and S2 of the Supporting Information. It is evident from the results that the dissociation pathway is similar for different pulling velocities. Hence, the pulling velocity of 0.004 nm/ps was selected for further simulation and also to explore proper conformational sampling.

The trajectories obtained from SMD simulations were used to extract 23 frames with increasing COM distance between the reference group and group being pulled with a step size of 0.5 Å. The extracted frames form the reaction coordinate ($\xi$) for the umbrella sampling simulations. Usually, the $\Delta G$ of a particular event (binding or dissociation) along a $\xi$ is calculated using US simulations. In this study, the $\xi$ is along the long axis of the CPNT ($z$ axis). The US simulations on each of the 391 umbrella sampling windows collected from 17 different SMD simulations were carried out for 10 ns. The total US simulation time was 3.91 $\mu$s. The WHAM method was used to derive the one-dimensional potential of mean force curves of each system from the US simulations.[58] The statistical error associated with the potential of mean force (PMF) calculation was carried out using the bootstrap analysis.[63]

## RESULTS AND DISCUSSION

**Structural Property.** Different structural properties of various systems ($(WL)_2$, $(WL)_8$, $(QAEA)_8$) in polar and nonpolar solvent environments have been derived from the classical MD simulation. It is found from results that the structural properties of CPNTs are affected by the different solvent environments as a result of the inherent nature of the side chains of different constituent amino acids. The root-mean-square deviation (rmsd) of the backbone and side chain heavy atoms with respect to the initial structure (after initial equilibration) is presented in Figure 1. It can be noted that the rmsd and its standard deviation for all systems is higher in the polar solvent than in the nonpolar solvent. Since $(WL)_2$ consists of two CP units, fluctuations in the rmsd are higher. The dynamic nature of the backbone atoms and the interaction of water molecules with the side chain of amino acids increase the rmsd values in the water medium; however, a decrease in these fluctuations can be observed in the nonpolar solvent as a result of the absence of H-bonding interactions between the carbonyl amide group and water molecules.

The angle ($\varphi$) formed by the alternate C$\alpha$ atoms of each CP unit provides information about the planarity. Thus, the deviation from planarity can be related to the twist in the CP unit. Figure 2 illustrates the probability of finding a particular $\varphi$ for various CPNTs. It can be seen that the equilibrium of $\varphi$ may vary substantially from 0° for the $(WL)^{aq}_2$ model, which indicates large deviations from planarity in the $(WL)^{aq}_2$ system. The distribution of $\varphi$ values for the $(WL)^{aq}_2$ and $(WL)^{aq}_8$ systems reveals that stacking of several CP units decreases the range of the distribution, as can be seen from Figure 2a and b. Thus there is an intrinsic relationship between the number of


dx.doi.org/10.1021/jp303418a | J. Phys. Chem. B 2012, 116, 9922−9933

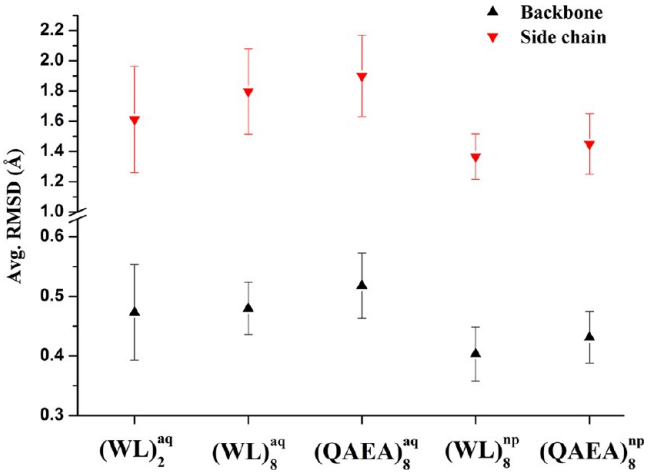


**Figure 1.** Average rmsd of backbone and side chain heavy atoms of various CPNTs with standard deviation.

stacked CP units and the $\varphi$ values. It is possible to note from the distribution function of $\varphi$ that the solvent medium does not significantly affect the $\varphi$ values.

**Hydrogen Bonding Interaction.** The donor−acceptor (DA) interatomic distance and donor−hydrogen−acceptor (DHA) angle criteria used to identify the existence of an H-bonding interaction are a DA distance of $\leq$3.5 Å and a DHA angle of $\geq$150°, respectively. The normalized frequency of occurrence of H-bonds between the backbone−backbone of various CPNTs in the last 5 ns of the MD simulation is shown in Figure 3. The same for the side chain−side chain H-bonds in the $(QAEA)_8$ model is given in Figure 4. Each CP unit can form eight unique backbone−backbone H-bonds with its adjacent CP unit, and thus, the dimer can form eight intermolecular H-bonds. The CPNTs with eight CP units can form 56 H-bonds. However, the number of H-bonds differs from the maximum possible value as a result of its dynamical nature. It can be seen from Figure 3 that the number of H-bonds decreases in an aqueous environment as a result of the interaction of water molecules with the backbone and the side chain atoms. It is apparent from Figure 4 that the presence of a polar side chain increases the H-bonding interaction with the water molecules. The number of Gln-Gln and Glu-Glu H-bond interactions decreases in the polar medium compared with the nonpolar environment. Thus, these H-bonds stabilize the systems in the nonpolar environment.

Figure 5 depicts the intermolecular H-bonding between the Gln-Gln and Glu-Glu side chains in the aqueous and nonpolar environment. Figures 5a and c illustrate the interaction of first shell water molecules with the side chains of the Gln and Glu residues. In the aqueous medium, the polar side chain interacts with the water molecules and formation of water-mediated H-bonded networks can be observed. In the nonpolar environment, the side chain of Gln reorients in a head-to-tail fashion to form side chain−side chain H-bonding (Figure 5b) interactions with the other Gln residue. In addition, the occurrence of H-bonding interactions with the side chain of Glu is higher than that of the Gln residue in the nonpolar solvent. Overall, it is clear that these CPNTs form more H-bonds between two CPs in the nonpolar solvent environment than in an aqueous medium.

**Steered Molecular Dynamics.** Since it has been shown that the backbone−backbone H-bonding and side chain−side chain interactions are responsible for the stability of CPNTs,[17−26] a single CP unit (or group of CP units) was (were) moved from the self-assembled CPs to unravel the dissociation mechanism. A series of conformations generated from the SMD simulation were further used for the US simulations.[64−66] The plot of the pulling force against time for various SMD simulations is presented in Figure 6. The maximum force observed for each SMD simulation indicates the point at which the breakdown of the critical interaction between the reference and pulling groups occurs. Here, the critical interaction refers to the intermolecular H-bond or hydrophobic interactions. As the path dependent mechanism of the breaking of the interaction between the reference group and the group being pulled is mediated by the solvent molecules, the comparison of the maximum pulling force for various systems does not yield a meaningful trend in the free energy of binding. Various interactions between the reference group, solvent, and the adjacent CP unit in the group being pulled have been analyzed for all model systems from the SMD simulation; the results are presented in Figure 7.

**Dissociation Pathway.** It is noticeable from Figure 6a that the pulling force profile for the $(WL)_{2\rightarrow1}^{aq}$ system deviates considerably from the other systems in such a way that the force decreases gradually from the maximum level. In accordance with the force profile of the $(WL)_{2\rightarrow1}^{aq}$ system, the number of backbone−backbone H-bond and side chain−side chain van der Waals contacts decreases steadily with the increase in force (Figure 7a). At the same time, the interaction of water molecules with the backbone polar groups increases. A small peak in the force vs. time plot at 62 ps corresponds to the reduction in the number of side chain van der Waals contacts and the backbone−backbone H-bonds. This is further confirmed by the increase in the COM distance (Figure 7a).

In contrast to the $(WL)_{2\rightarrow1}^{aq}$ system, the number of backbone−backbone H-bonds in the $(WL)_{8\rightarrow1}^{aq}$ system shows marginal fluctuations until the maximum force is reached. After attaining the maximum force, the breaking of the backbone−backbone H-bonds takes place within 6 ps. In the case of the $(WL)_{2\rightarrow1}^{aq}$ system, the breaking of backbone−backbone H-bonds occurs before the maximum force. On the other hand, the $(WL)_{8\rightarrow1}^{aq}$ system's backbone−backbone H-bonds break only after the maximum force has been applied. The process of breaking various interactions between the reference group and the group being pulled was calculated, and results are presented in Table 1. It is evident from Table 1 that the transition time for the complete breaking of van der Waals contacts after attaining the maximum force is considerably higher for the $(WL)_{2\rightarrow1}^{aq}$ system when compared with the $(WL)_{8\rightarrow1}^{aq}$ system. In the $(WL)_{2\rightarrow1}^{aq}$ system, the van der Waals contacts exist for ~41 ps after attaining the maximum force. On the other hand, the same interaction persists only for 14 ps in the $(WL)_{8\rightarrow1}^{aq}$ system.

The normalized distribution functions of $\varphi$ for various pulling groups from the SMD simulation are presented in Figure S3 of the Supporting Information. It is evident from the twist angles that the $(WL)_{2\rightarrow1}^{aq}$ system undergoes a large conformational twist in the dissociation pathway. The snapshots taken from the dissociation pathways of the $(WL)_{2\rightarrow1}^{aq}$, $(WL)_{8\rightarrow1}^{aq}$, and $(WL)_{8\rightarrow4}^{aq}$ systems are presented in Figure 8a and b and Figure S4 in the Supporting Information. It can be found that the conformational twist is observed in the pulling group of the dimer $(WL)_{2\rightarrow1}^{aq}$ system. A comparison of the dissociation pathways of the $(WL)_{2\rightarrow1}^{aq}$ and $(WL)_{8\rightarrow1}^{aq}$ systems reveals that the dissociation of one CP unit from the $(WL)_{8\rightarrow1}^{aq}$ system is


dx.doi.org/10.1021/jp303418a | J. Phys. Chem. B 2012, 116, 9922−9933

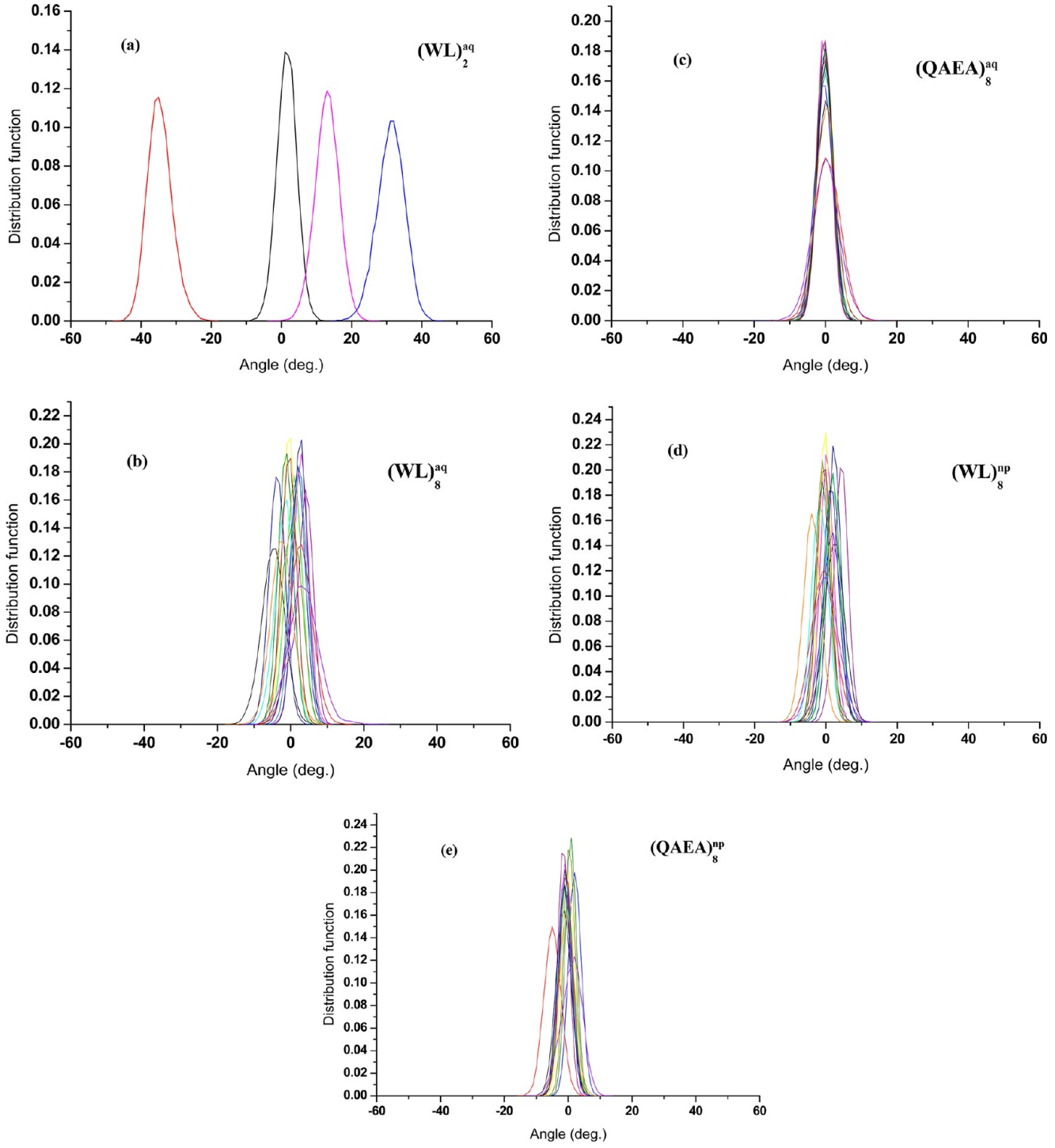


**Figure 2.** Normalized distribution of the alternate C$\alpha$ atom dihedral angles ($\varphi$) in each CP unit of various CPNTs.

achieved by collective breaking of the interactions. The multiple stacking of CPs plays a major role in the dissociation pathway and thus provides additive stability to the self-assembly process.

In the case of the octamer systems, the breaking of the backbone−backbone H-bond is followed by the annihilation of van der Waals contacts between the side chains. After attaining the maximum force, the backbone H-bonds remain for 6−23 ps and the side chain van der Waals contacts survive for 6−35 ps (Table 1 and Figure 7). The pulling of a monomer and dimer shows a gradual increase in the COM distance, and at the same time, a steady decrease in the number of van der Waals contacts can be observed. The pulling of a trimer and tetramer demonstrates minimal fluctuations in the COM distance and van der Waals interactions until the maximum force is achieved. In the nonpolar solvent, the side chain H-bonds and the van der Waals contacts of the $(QAEA)_{8\rightarrow 1-4}^{np}$ systems exhibit only marginal fluctuations (Figure 7n−q). The pulling force of the $(WL)_{8\rightarrow 1-4}^{aq}$ systems is substantially higher than the $(QAEA)_{8\rightarrow 1-4}^{aq}$ systems in the aqueous medium (Figure 6). In the presence of a nonpolar solvent, the favorable solvation effect observed by the nonpolar side chains reduces the pulling force of the $(WL)_{8\rightarrow 1-4}^{np}$ systems with respect to $(QAEA)_{8\rightarrow 1-4}^{np}$


dx.doi.org/10.1021/jp303418a | J. Phys. Chem. B 2012, 116, 9922−9933

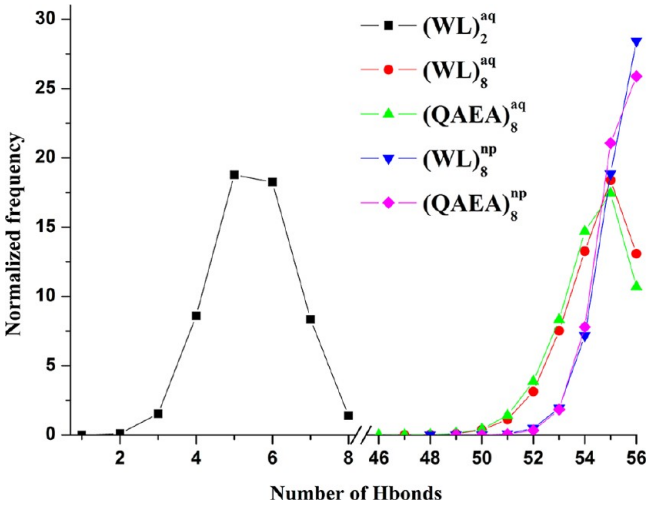


**Figure 3.** Normalized frequency of backbone−backbone H-bonds observed in various systems.

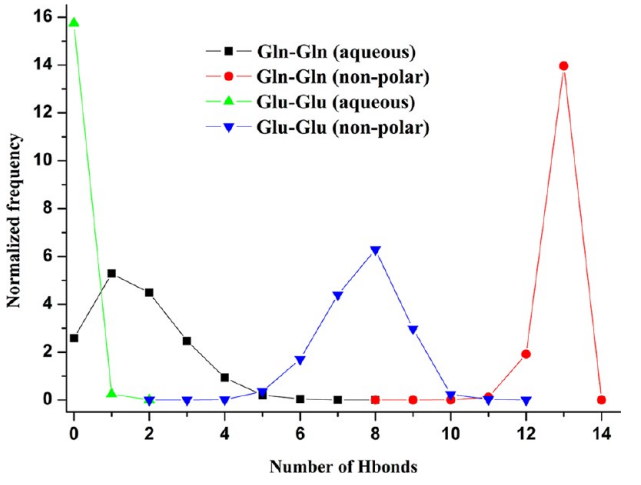


**Figure 4.** Normalized frequency of H-bonds between various side chains of the $(QAEA)_8$ system in polar and nonpolar environments.

systems. In addition, the unfavorable solvation of the backbone carbonyl amide functionality remarkably increases the pulling force in the nonpolar solvent.

In an aqueous medium, the increase in the COM distance and associated decrease in the backbone−backbone H-bonds or side chain van der Waals contacts provide accessibility for water molecules to interact with the backbone polar groups. Figure 7b−i shows that the gain of accessibility of water molecules to the backbone polar groups varies from the $(WL)^{aq}_{8\rightarrow1-4}$ to $(QAEA)^{aq}_{8\rightarrow1-4}$ systems. The accessibility of water molecules in the $(WL)^{aq}_{8\rightarrow1-4}$ systems from the surface of the tube is hindered by the bulky side chains of Trp residues while the backbone polar groups of the $(QAEA)^{aq}_{8\rightarrow1-4}$ systems interact with water molecules from the surface as well as from the lumen of the tube. Thus, it increases the solvation of the backbone when compared with that of the $(WL)^{aq}_{8\rightarrow1-4}$ systems. A similar observation has been found from a previous MD study.[38]

The twist angle calculated for various pulling groups reflects the changes in the distribution of $\varphi$ from pulling of monomer to tetramer units (Figure S3 in the Supporting Information). The dihedral angle distribution in a nonpolar environment is comparatively smaller than in the aqueous medium. It is evident

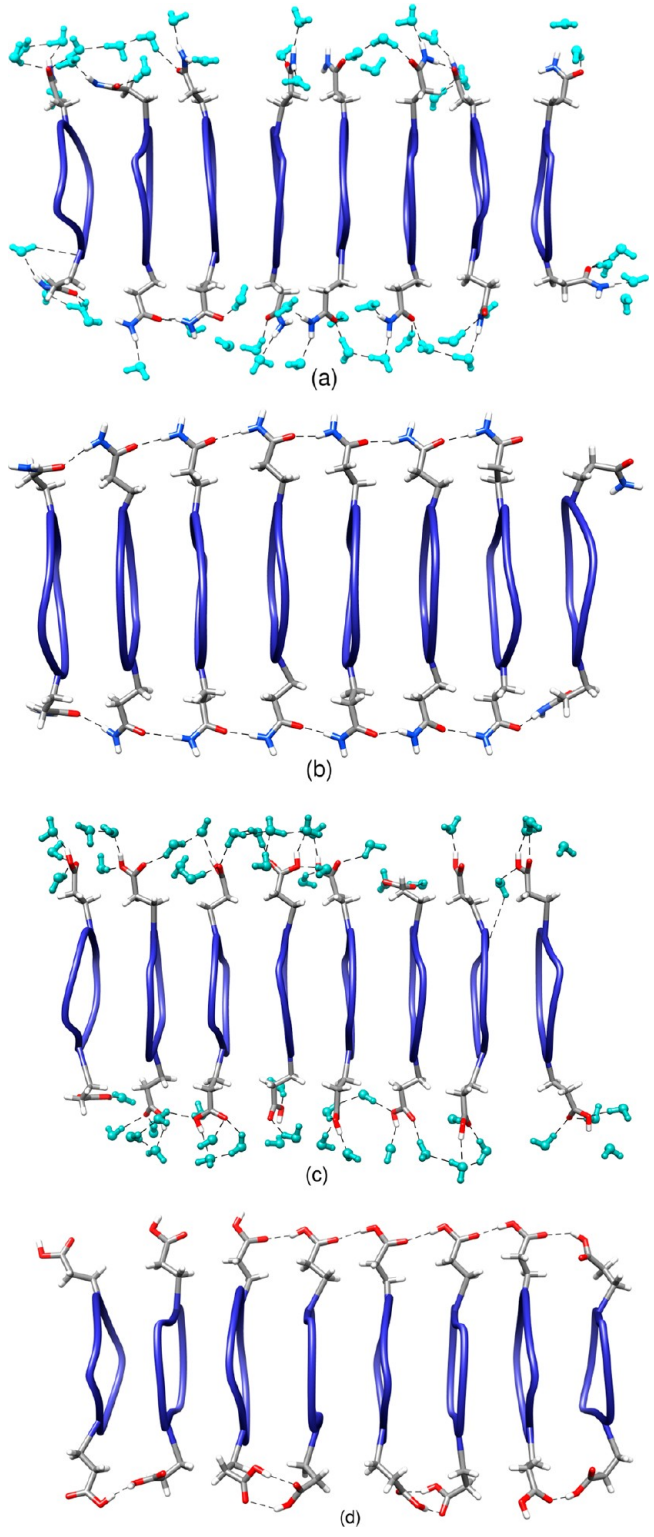


**Figure 5.** H-bonding (dashed lines) between Gln-Gln (a, b) and Glu-Glu (c, d) residues of the $(QAEA)_8$ system in polar (a, c) and nonpolar (b, d) environments. The water molecules are shown as cyan ball and stick representations. The main chain atoms are shown as ribbons, and to enhance the visibilty, Ala residues are not shown.

from the twist angle distribution that the monomer and dimer (pulling groups) undergo large conformational changes in the reaction path. Hence, the dissociation process is carried out by a gradual breaking of contacts between the reference group and


dx.doi.org/10.1021/jp303418a | J. Phys. Chem. B 2012, 116, 9922−9933

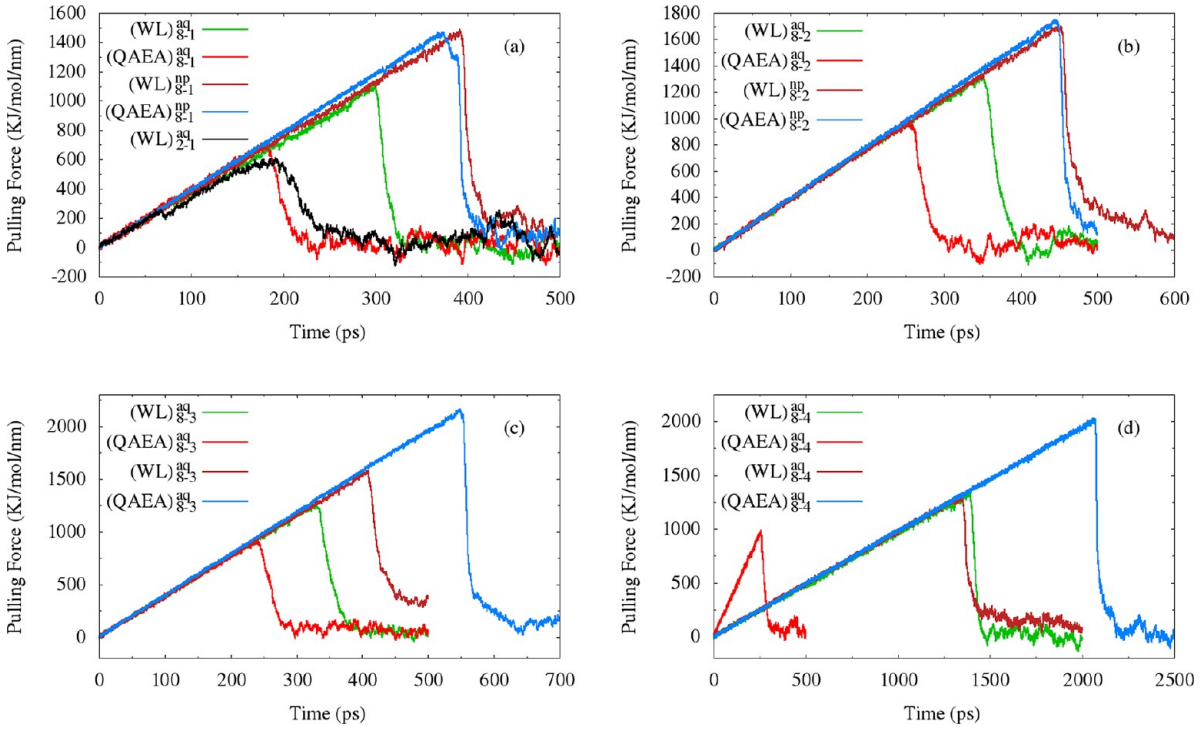


**Figure 6.** The pulling force vs. time of various systems in polar and nonpolar environments.

the group being pulled. This characteristic dissociation path is confirmed by the steady decrease in the backbone−backbone H-bonds and side chain van der Waals contacts. The annihilation time of various interactions between the reference group and the group being pulled and the corresponding COM distance (Table 1) demonstrate that the first phase of the breaking event is controlled by the backbone−backbone H-bonds. The COM distance corresponding to the complete annihilation of H-bonds and van der Waals contacts decreases from monomer to tetramer CP pulling (Table 1). Figure 8b and c illustrates the difference in the dissociation pathway of the $(WL)^{aq}_{8\rightarrow1}$ and $(WL)^{aq}_{8\rightarrow4}$ systems. The decrease in the twist angle from monomer to oligomeric pulling units and the COM distance at which there is complete annihilation of H-bonds demonstrates that the dissociation of the trimer and tetramer are not facilitated by the stepwise breaking of various interactions between the reference and pulling groups. In these cases, breaking of several contacts takes place within a short time span, and thus, dissociation requires more force.

**Free Energy of Binding.** The PMF curves obtained from the US simulation are presented in Figure 9. The calculated free energy of binding ($\Delta G_{binding}$) for various systems is listed in Table 2. The energy minima for various systems vary as a function of the number of CP units in the group being pulled. Both the occurrence of energy minima on the PMF curves and the corresponding COM distance depend on various side chains and associated side chain−side chain interaction (hindrance). The COM distance corresponding to the energy minimum is presented in Table S1 of the Supporting Information. The energy minima for the $(WL)^{aq/np}_{8\rightarrow1-4}$ systems are observed at slightly higher COM distance than the $(QAEA)^{aq/np}_{8\rightarrow1-4}$ systems as a result of the presence of the bulky side chain hindrance in the $(WL)^{aq/np}_{8\rightarrow1-4}$ systems. The COM distance corresponding to the energy minima of the $(WL)^{aq/np}_{8\rightarrow1-4}$ systems does not show appreciable changes in polar and nonpolar solvents. The simulation of the $(QAEA)^{np}_{8\rightarrow1}$ system in the nonpolar environment considerably reduces the COM distance corresponding to the energy minima.

Despite the observable differences in the dissociation pathways of the $(WL)^{aq}_{2\rightarrow1}$ and $(WL)^{aq}_{8\rightarrow1}$ systems, the free energy of binding of the $(WL)^{aq}_{2\rightarrow1}$ system is marginally lower than the $(WL)^{aq}_{8\rightarrow1}$ system; however, the energy minimum for the $(WL)^{aq}_{2\rightarrow1}$ system occurs at a slightly higher COM distance when compared with that in the $(WL)^{aq}_{8\rightarrow1}$ system (Figure 9). Considering the error in the free energy of binding of the $(WL)^{aq}_{8\rightarrow1}$, $(WL)^{aq}_{8\rightarrow2}$, $(QAEA)^{aq}_{8\rightarrow1}$, and $(QAEA)^{aq}_{8\rightarrow2}$ systems, neither monomer nor dimer shows appreciable changes in the aqueous medium (Table 2). In addition, the accessibility of water molecules from the surface of the tube and the favorable solvation of polar side chains in the $(QAEA)^{aq}_{8\rightarrow1-4}$ systems considerably affects the intermolecular interactions. As a consequence, it decreases the free energy of binding.

The nonpolar nature of the side chains of the $(WL)^{aq}_{8\rightarrow1-4}$ systems produces an unfavorable solvation effect in the aqueous medium and at the same time increases the side chain−side chain stacking interaction. The bulky nature of the Trp side chain in the $(WL)^{aq}_{8\rightarrow1-4}$ system reduces the accessibility of water molecules to the backbone polar groups from the surface of the tube, and hence, backbone−backbone H-bonding is less affected in the $(WL)^{aq}_{8\rightarrow1-4}$ systems. It can be noted that in the polar solvent, the backbone or side chain polar groups in the dissociating CP units of $(QAEA)^{aq}_{8\rightarrow1-4}$ are further stabilized by the favorable solvation effect. The trimer interaction energy in the polar solvent is substantially increased due to the favorable stacking interaction. It is evident from Table 2 that the free energy of binding for the $(WL)^{aq}_{8\rightarrow1-4}$ systems is comparatively higher than that for the $(QAEA)^{aq}_{8\rightarrow1-4}$ systems. The reduced free energy of binding for the $(QAEA)^{aq}_{8\rightarrow1-4}$ systems is justified by two facts: (a) the favorable solvation effect of the polar side chains and (b) the presence of Ala residues confers water


dx.doi.org/10.1021/jp303418a | J. Phys. Chem. B 2012, 116, 9922−9933

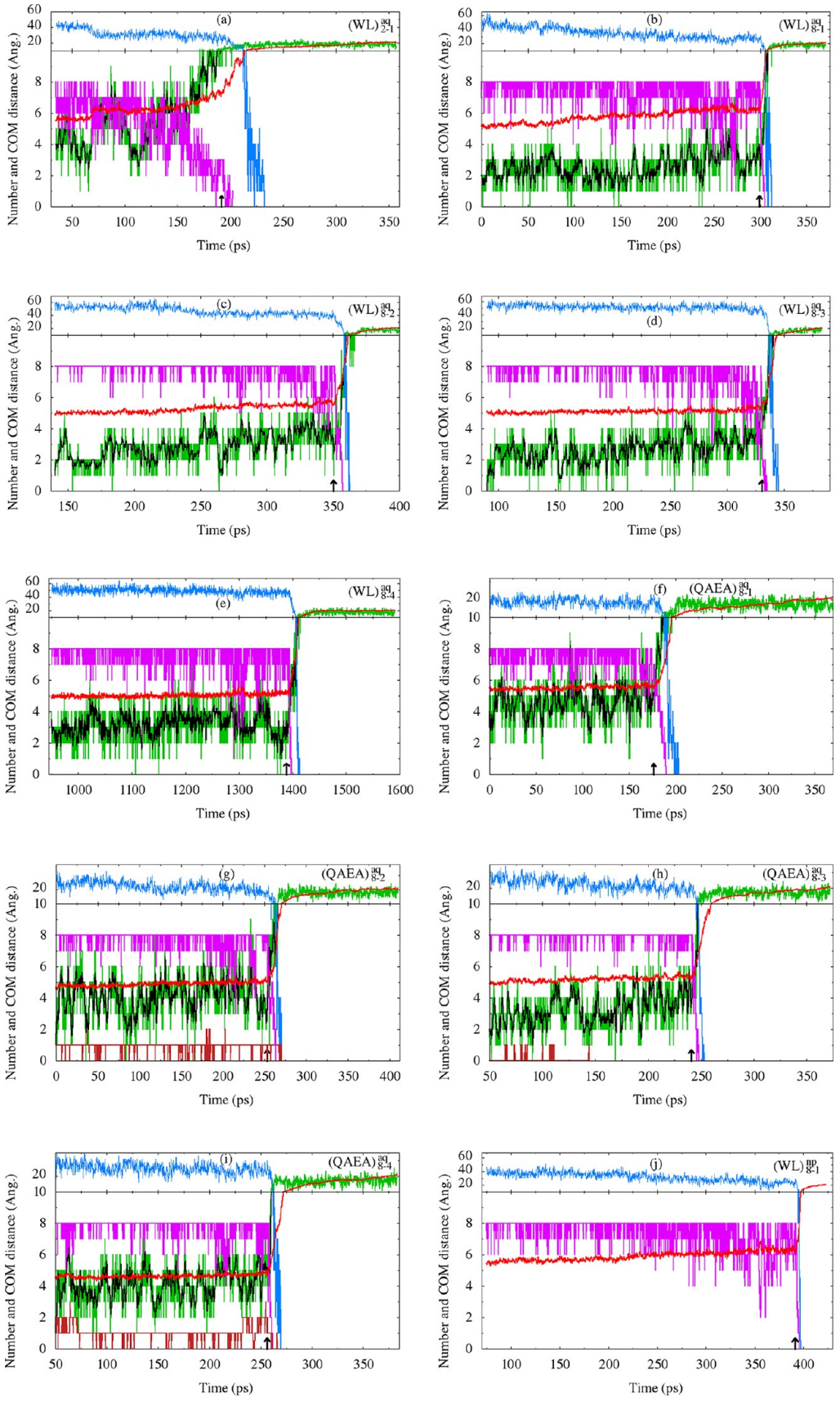


**Figure 7.** continued


dx.doi.org/10.1021/jp303418a | J. Phys. Chem. B 2012, 116, 9922−9933

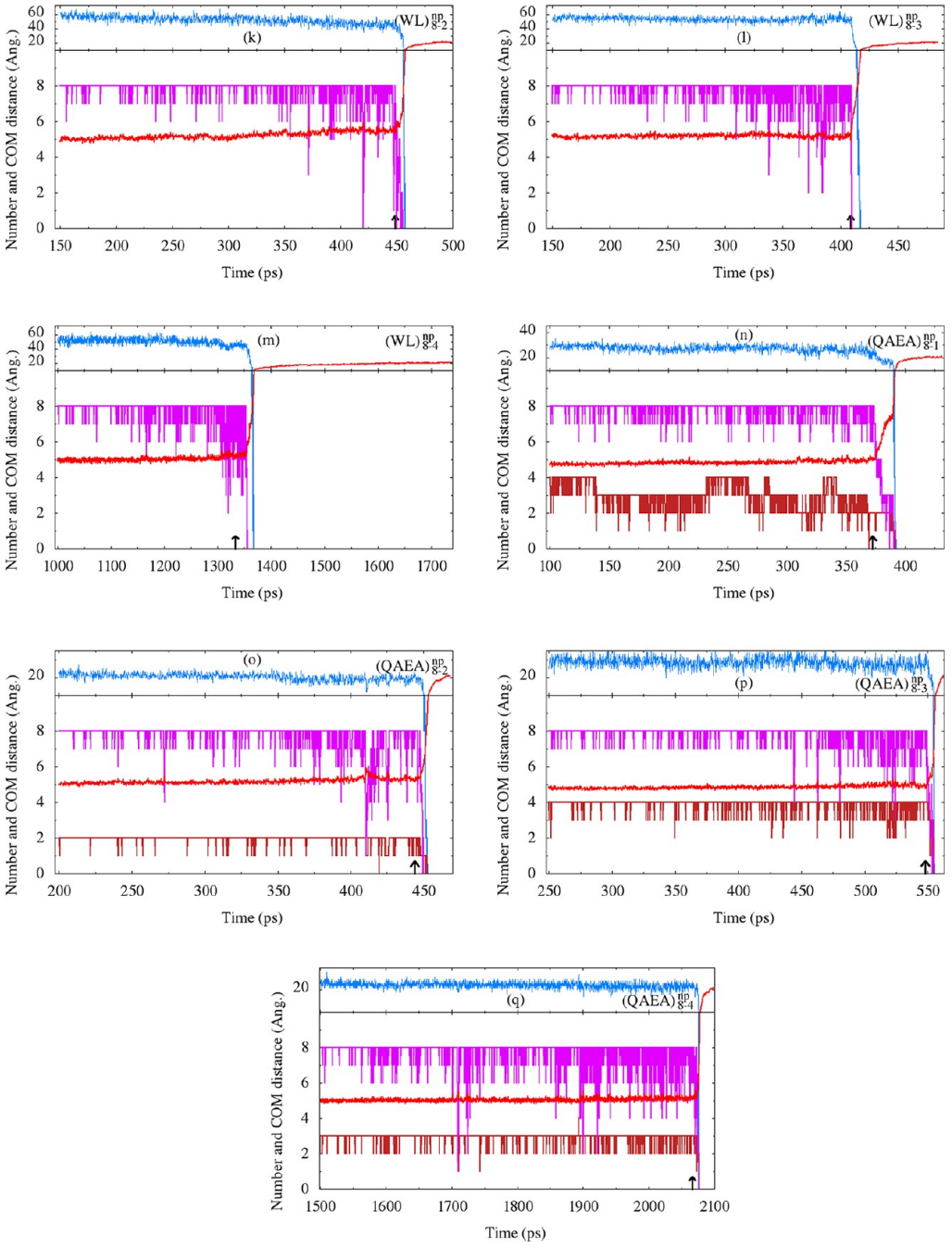


**Figure 7.** Various interactions between the reference group and groups being pulled as a function of the COM distance (in angstroms, red) between the reference and adjacent CP unit in the group being pulled as obtained from the SMD simulation. Number of H-bonds: backbone−backbone (magenta), backbone−water (green), backbone−water running average (window size = 5, black), side chain−side chain (brown). Number of van der Waals contacts: side chian−side chain (blue). The arrow in the *x* axis shows the time at which force reaches its maximum value.

molecules access to the backbone polar groups from the surface of the tube.

In the presence of a nonpolar solvent, the free energy of binding for the monomer unit is substantially higher than the dimer due to the unfavorable solvation effect of the carbonyl amide groups. Furthermore, the presence of side chain polar groups significantly increases the free energy of binding for the $(QAEA)^{np}_{8\rightarrow 1}$ system. The saturation point for the free energy of binding of the $(WL)^{np}_{8\rightarrow 1-4}$ systems is attained from the trimer CP unit as a result of the stabilization of dissociating groups by backbone−backbone H-bonding and various side chain−side chain interactions. In the case of the $(QAEA)^{np}_{8\rightarrow 1-4}$ systems, the difference in the free energy of binding for $(QAEA)^{np}_{8\rightarrow 2}$ and $(QAEA)^{np}_{8\rightarrow 3}$ systems is 18.91 kcal/mol. On the other hand, the difference between the free energies of the $(QAEA)^{np}_{8\rightarrow 3}$ and $(QAEA)^{np}_{8\rightarrow 4}$ systems is 5.51 kcal/mol. It can be noted that the saturation point in the free energy of binding of $(QAEA)^{np}_{8\rightarrow 1-4}$ systems is 2-fold higher than the $(WL)^{np}_{8\rightarrow 1-4}$ systems. The strong electrostatic interaction between the side chains and unfavorable solvation effects increases the saturation point in the free energy of binding of $(QAEA)^{np}_{8\rightarrow 1-4}$ systems. At the same time, the favorable solvation effect of the $(WL)^{np}_{8\rightarrow 1-4}$ system side chains in the nonpolar solvent does not enhance the free energy of binding. The $(QAEA)^{np}_{8\rightarrow 1-4}$ systems are


dx.doi.org/10.1021/jp303418a | *J. Phys. Chem. B* 2012, 116, 9922−9933

**Table 1. SMD Simulation Time at Which the Pulling Force Reaches Maximum Value for Various Model Systems[a]**

| system | time (ps) | max force (kJ/mol/nm) | H-bonds[b] (ps) | vdW contact[b] (ps) | H-bonds COM distance[c] (Å) | vdW COM distance[c] (Å) |
|---|---|---|---|---|---|---|
| $(WL)^{aq}_{2\rightarrow1}$ | 191.4 | 611.56 | 202.8 | 232.0 | 8.62 | 12.88 |
| $(WL)^{aq}_{8\rightarrow1}$ | 298.8 | 1105.77 | 304.8 | 312.4 | 8.87 | 14.03 |
| $(WL)^{aq}_{8\rightarrow2}$ | 350.4 | 1341.13 | 357.0 | 362.6 | 7.28 | 10.04 |
| $(WL)^{aq}_{8\rightarrow3}$ | 330.4 | 1266.59 | 334.8 | 345.0 | 5.75 | 10.53 |
| $(WL)^{aq}_{8\rightarrow4}$ | 1388.0 | 1344.25 | 1398.4 | 1413.6 | 6.06 | 10.20 |
| $(QAEA)^{aq}_{8\rightarrow1}$ | 176.8 | 711.29 | 189.6 | 203.2 | 7.22 | 11.38 |
| $(QAEA)^{aq}_{8\rightarrow2}$ | 253.0 | 996.27 | 263.4 | 270.2 | 6.64 | 9.80 |
| $(QAEA)^{aq}_{8\rightarrow3}$ | 240.4 | 920.47 | 248.0 | 252.6 | 6.97 | 8.39 |
| $(QAEA)^{aq}_{8\rightarrow4}$ | 256.2 | 986.93 | 260.8 | 269.8 | 5.73 | 8.64 |
| $(WL)^{np}_{8\rightarrow1}$ | 391.2 | 1490.62 | 395.4 | 397.0 | 7.60 | 9.46 |
| $(WL)^{np}_{8\rightarrow2}$ | 449.0 | 1715.39 | 455.2 | 457.8 | 6.42 | 9.81 |
| $(WL)^{np}_{8\rightarrow3}$ | 409.0 | 1575.25 | 409.8 | 417.4 | 5.60 | 9.61 |
| $(WL)^{np}_{8\rightarrow4}$ | 1333.2 | 1307.79 | 1356.2 | 1367.8 | 5.86 | 9.54 |
| $(QAEA)^{np}_{8\rightarrow1}$ | 372.4 | 1468.57 | 390.8 | 392.2 | 8.61 | 11.35 |
| $(QAEA)^{np}_{8\rightarrow2}$ | 444.2 | 1749.44 | 450.0 | 452.6 | 6.03 | 8.80 |
| $(QAEA)^{np}_{8\rightarrow3}$ | 548.2 | 2159.07 | 554.2 | 555.2 | 6.02 | 8.10 |
| $(QAEA)^{np}_{8\rightarrow4}$ | 2066.2 | 2028.63 | 2075.6 | 2076.8 | 6.17 | 7.86 |

[a]The simulation time and COM distance corresponding to the annihilation of backbone−backbone H-bonds and side chain−side chain van der Waals contacts between the reference group and adjacent CP unit in the group being pulled. [b]Complete breaking time of backbone−backbone H-bonds and side chain−side chain van der Waals (vdW) contact. [c]COM distance between the reference group and the adjacent CP unit of the group being pulled at which the H-bonds and vdW contacts become 0.

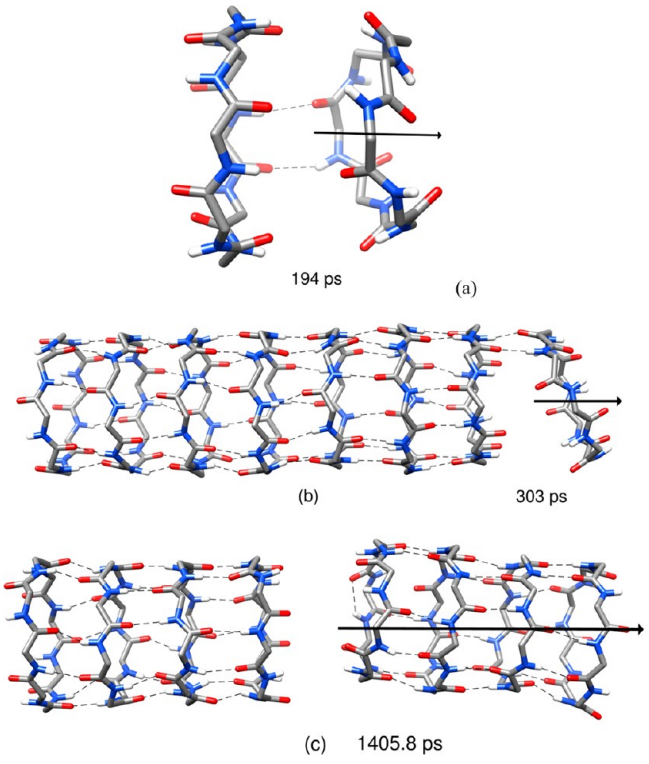


**Figure 8.** Snapshots of (a) $(WL)^{aq}_{2\rightarrow1}$, (b) $(WL)^{aq}_{8\rightarrow1}$, and (c) $(WL)^{aq}_{8\rightarrow4}$ systems corresponding to 7.5 Å COM distance between the reference group and the adjacent CP unit of the group being pulled as observed from the SMD simulation. The pulling direction is shown as a solid arrow. The backbone−backbone H-bonding is represented as dashed lines, and for clear visibility, the side chains are not shown.

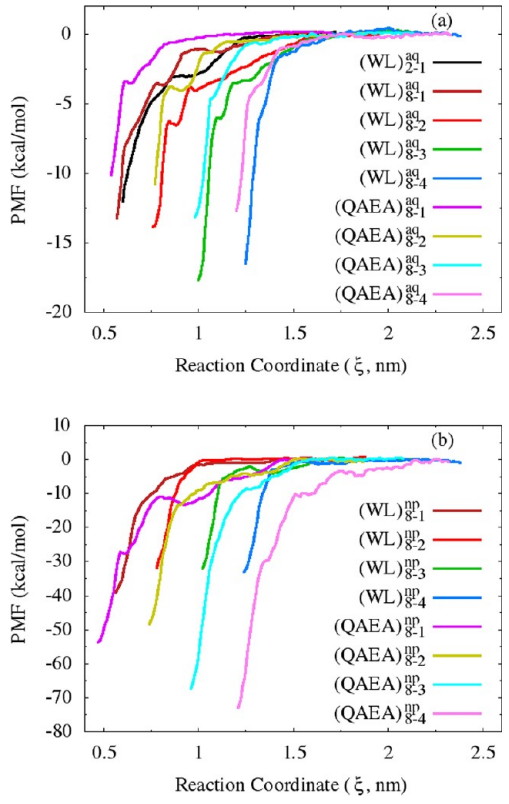


**Figure 9.** Potential of mean force (PMF) curves of various systems in polar (a) and nonpolar (b) solvents.

much more stable in the nonpolar solvent in comparison with that of the $(WL)^{np}_{8\rightarrow1-4}$ systems. The opposite is true in the aqueous medium.

The enthalpic contribution of each intermolecular H-bonding interaction in $\{cyclo[(\text{L-Phe-D-}N\text{-MeAla})_4]\}_2$ is predicted as 0.5−0.7 kcal/mol in chloroform.[23] It is evident from the enthalpic contribution of each H-bond that the dimer model system contains eight intermolecular H-bonds that can contribute 4.0−5.6 kcal/mol for the dimerization in chloroform.[23] Using the Jarzynski's equality method, the free energy of binding for the $\{cyclo[(\text{L-Trp-D-}N\text{-MeLeu})_4]\}_2$ system has been calculated as 7 ± 1 kcal/mol in nonane.[56] The reported enthalpic contribution and free energy of binding are calculated


dx.doi.org/10.1021/jp303418a | J. Phys. Chem. B 2012, 116, 9922−9933

**Table 2. The Binding Free Energies (kcal/mol) and Standard Deviations of Various Groups of CPs in the Self-Assembly Process in Polar and Nonpolar Environments**

| system | $\Delta G_{binding}$ | system | $\Delta G_{binding}$ |
|---|---|---|---|
| $(WL)^{aq}_{2\rightarrow1}$ | −12.30 (0.33) | | |
| $(WL)^{aq}_{8\rightarrow1}$ | −13.37 (0.35) | $(WL)^{np}_{8\rightarrow1}$ | −39.20 (0.59) |
| $(WL)^{aq}_{8\rightarrow2}$ | −13.90 (0.28) | $(WL)^{np}_{8\rightarrow2}$ | −32.22 (0.42) |
| $(WL)^{aq}_{8\rightarrow3}$ | −17.83 (0.43) | $(WL)^{np}_{8\rightarrow3}$ | −32.40 (0.37) |
| $(WL)^{aq}_{8\rightarrow4}$ | −16.94 (0.37) | $(WL)^{np}_{8\rightarrow4}$ | −33.29 (0.82) |
| $(QAEA)^{aq}_{8\rightarrow1}$ | −10.41 (0.25) | $(QAEA)^{np}_{8\rightarrow1}$ | −54.01 (0.81) |
| $(QAEA)^{aq}_{8\rightarrow2}$ | −11.26 (0.29) | $(QAEA)^{np}_{8\rightarrow2}$ | −48.63 (0.71) |
| $(QAEA)^{aq}_{8\rightarrow3}$ | −13.24 (0.42) | $(QAEA)^{np}_{8\rightarrow3}$ | −67.54 (0.87) |
| $(QAEA)^{aq}_{8\rightarrow4}$ | −12.72 (0.38) | $(QAEA)^{np}_{8\rightarrow4}$ | −73.05 (0.93) |

for the N-methylated dimer. Because of the favorable solvation effect of the N-methylated CPs in the nonpolar solvent, the reported free energy of binding values are considerably lower than the observed values from the current study.

## CONCLUSIONS

The present study has investigated the structure, dissociation pathway, and stability of self-assembled CPs composed of *cyclo*-[(D-Trp-L-Leu)$_4$] and *cyclo*-[(L-Gln-D-Ala-L-Glu-D-Ala)$_2$] in polar and nonpolar solvents using classical, steered MD and US simulations. The calculated rmsd values confirm that CPNTs undergo less fluctuation in the nonpolar solvent than the polar solvent. Intermolecular H-bonding interactions are more consistent in the nonpolar solvent medium than in the polar solvent. The solvent effect plays a dominant role in the dissociation of CPs from the CPNT. The pulling force for dissociation of various CPs from the $(WL)_8$ system is considerably higher in an aqueous medium when compared with a nonpolar medium. In the case of the $(QAEA)_8$ system, the presence of polar side chains decreases the required pulling force in the polar solvent compared with the nonpolar solvent. The accessibility of water molecules to the backbone carbonyl amide groups from the surface of the tube enhances the dissociation process.

The comparison of dissociation pathways of a monomer CP unit from the $(WL)^{aq}_2$ and $(WL)^{aq}_8$ systems reveals that stacking of multiple CPs induces mechanical stability to the self-assembled CPs; however, it does not influence the calculated free energy of binding of $(WL)^{aq}_2$ in comparison with $(WL)^{aq}_8$ because of the solvation effect. The cooperativity in the breaking of various interactions between the reference group and group being pulled increases from $CP_1$ to $CP_4$. Thus, the cooperative breaking event requires substantially higher pulling force. The $(WL)^{aq}_{8\rightarrow1-4}$ systems are more stable than $(QAEA)^{aq}_{8\rightarrow1-4}$ systems in an aqueous medium because of the lower solubility of side chains. It is evident from the results that the selected CPNTs are highly stable in the nonpolar solvent than in the polar solvent. The complementary solvation effect of side chains plays a major role in the stability of CPNTs. Hence, the CPNTs composed of polar and nonpolar amino acids could retain moderate stability in both polar and nonpolar environments.

## ASSOCIATED CONTENT

### Supporting Information

COM distance between the reference group and the group being pulled at which the energy minima on PMF curves of various systems occurs, force vs. time plot for different pulling velocities, dissociation pathway of the $(WL)^{aq}_{8\rightarrow1}$ system using different velocities, normalized distribution of the $\varphi$ angles in each CP unit of groups being pulled in various systems, dissociation pathway of the $(WL)^{aq}_{2\rightarrow1}$ and $(WL)^{aq}_{8\rightarrow1}$ systems in polar solvent, and the complete list of authors for references 41 and 49. This material is available free of charge via the Internet at http://pubs.acs.org.

## AUTHOR INFORMATION

### Corresponding Author

*E-mail: subuchem@hotmail.com.

### Notes

The authors declare no competing financial interest.

## ACKNOWLEDGMENTS

We thank the Council of Scientific and Industrial Research (CSIR), New Delhi, for financial assistance. R.V. is grateful to the Erasmus Mundus External Cooperation Window Lot 13, Eurindia project for financial assistance. We are thankful to the ICT Department of Ghent University for assistance with the computations.

## REFERENCES

(1) Lewis, J. P.; Pawley, N. H.; Sankey, O. F. *J. Phys. Chem. B* **1997**, *101*, 10576−10583.
(2) Jishi, R. A.; Flores, R. M.; Valderrama, M.; Lou, L.; Bragin, J. *J. Phys. Chem. A* **1998**, *102*, 9858−9862.
(3) Sanchez-Quesada, J.; Ghadiri, M. R.; Bayley, H.; Braha, O. *J. Am. Chem. Soc.* **2000**, *122*, 11757−11766.
(4) Asthagiri, D.; Bashford, D. *Biophys. J.* **2002**, *82*, 1176−1189.
(5) Sanchez-Quesada, J.; Isler, M. P.; Ghadiri, M. R. *J. Am. Chem. Soc.* **2002**, *124*, 10004−10005.
(6) Tarek, M.; Maigret, B.; Chipot, C. *Biophys. J.* **2003**, *85*, 2287−2298.
(7) Ferrante, F.; Manna, G. L. *J. Mol. Struct: THEOCHEM* **2003**, *634*, 181−186.
(8) Horne, W. S.; Wiethoff, C. M.; Cui, C.; Wilcoxen, K. M.; Amorin, M.; Ghadiria, M. R.; Nemerow, G. R. *Bioorg. Med. Chem.* **2005**, *13*, 5145−5153.
(9) Hwang, H.; Schatz, G. C.; Ratner, M. A. *J. Phys. Chem. B* **2006**, *110*, 6999−7008.
(10) Hwang, H.; Schatz, G. C.; Ratner, M. A. *J. Phys. Chem. B* **2006**, *110*, 26448−26460.
(11) Dehez, F.; Tarek, M.; Chipot, C. *J. Phys. Chem. B* **2007**, *111*, 10633−10635.
(12) Zhu, J.; Cheng, J.; Liao, Z.; Lai, Z.; Liu, B. *J. Comput. Aided Mol. Des.* **2008**, *22*, 773−781.
(13) Khalfa, A.; Treptow, W.; Maigret, B.; Tarek, M. *Chem. Phys.* **2009**, *358*, 161−170.
(14) Cheng, J.; Zhu, J.; Liu, B.; Liao, Z.; Lai, Z. *Mol. Simul.* **2009**, *35*, 625−630.
(15) Liu, H.; Chen, J.; Shen, Q.; Fu, W.; Wu, W. *Mol. Pharmaceutics* **2010**, *7*, 1985−1994.
(16) Liu, J.; Fan, J.; Tang, M.; Zhou, W. *J. Phys. Chem. A* **2010**, *114*, 2376−2383.
(17) Hassal, C. H. In *Chemistry and Biology of Peptides: Proceedings of the Third American Peptide Symposium*; Meinhoffer, J., Ed.; Ann Arbor Science: Ann Arbor, MI, 1972; pp 153−157.
(18) De Santis, P.; Morosetti, S.; Rizzo, R. *Macromolecules* **1974**, *7*, 52−58.
(19) Karle, I. L.; Handa, B. K.; Hassall, C. H. *Acta Crystallogr.* **1975**, *B 31*, 555−560.
(20) Tomasi, L.; Lorenzi, G. P. *Helv. Chim. Acta* **1987**, *70*, 1012−1016.
(21) Ghadiri, M. R.; Granja, J. R.; Milligan, R. A.; McRee, D. E.; Khazanovich, N. *Nature* **1993**, *366*, 324−327.

(22) Pavone, V.; Benedetti, E.; Di Blasio, B.; Lombardi, A.; Pedone, C.; Lorenzi, G. P. *Biopolymers* **1993**, *28*, 215−223.
(23) Ghadiri, M. R.; Kobayashi, K.; Granja, J. R.; Chadha, R. K.; McRee, D. E. *Angew. Chem., Int. Ed. Engl.* **1995**, *34*, 93−95.
(24) Hartgerink, J. D.; Granja, J. R.; Milligan, R. A.; Ghadiri, M. R. *J. Am. Chem. Soc.* **1996**, *118*, 43−50.
(25) Hartgerink, J. D.; Clark, T. D.; Ghadiri, M. R. *Chem.—Eur. J.* **1998**, *4*, 1367−1372.
(26) Bong, D. T.; Clark, T. D.; Granja, J. R.; Ghadiri, M. R. *Angew. Chem., Int. Ed.* **2001**, *40*, 988−1011.
(27) Khazanovich, N.; Granja, J. R.; McRee, D. E.; Milligan, R. A.; Ghadiri, M. R. *J. Am. Chem. Soc.* **1994**, *116*, 6011−6012.
(28) Ghadiri, M. R.; Granja, J. R.; Buehler, L. K. *Nature* **1994**, *369*, 301−304.
(29) Granja, J. R.; Ghadiri, M. R. *J. Am. Chem. Soc.* **1994**, *116*, 10785−10786.
(30) Gailer, C.; Feigel, M. *J. Comput.-Aided Mol. Des.* **1997**, *11*, 273−277.
(31) Chen, G.; Su, S.; Liu, R. *J. Phys. Chem. B* **2002**, *106*, 1570−1575.
(32) Qu, W.; Tan, H.; Chen, G.; Liu, R. *Int. J. Quantum Chem.* **2010**, *110*, 1648−1659.
(33) Clark, T. D.; Buehler, L. K.; Ghadiri, M. R. *J. Am. Chem. Soc.* **1998**, *120*, 651−656.
(34) Kim, H. S.; Hartgerink, D.; Ghadiri, M. R. *J. Am. Chem. Soc.* **1998**, *120*, 4417−4424.
(35) Liu, J.; Fan, J.; Tang, M.; Cen, M.; Yan, J.; Liu, Z.; Zhou, W. *J. Phys. Chem. B* **2010**, *114*, 12183−12192.
(36) Motesharei, K.; Ghadiri, M. R. *J. Am. Chem. Soc.* **1997**, *119*, 11306−11312.
(37) Tan, H.; Qu, W.; Chen, G. *Int. J. Quantum Chem.* **2005**, *102*, 1106−1115.
(38) Vijayaraj, R.; Raman, S. S.; Kumar, R. M.; Subramanian, V. *J. Phys. Chem. B* **2010**, *114*, 16574−16583.
(39) Jorgensen, W. L. *J. Am. Chem. Soc.* **1981**, *103*, 335−340.
(40) Jorgensen, W. L.; Chandrasekhar, J.; Madura, J. D.; Impey, R. W.; Klein, M. L. *J. Chem. Phys.* **1983**, *79*, 926−935.
(41) Case, D. A.; Darden, T. A.; Cheatham, T. E., III; Simmerling, C. L.; Wang, J.; Duke, R. E.; Luo, R.; Walker, R. C.; Zhang, W.; Merz, K. M. et al. *AMBER 11*; University of California: San Francisco, 2010.
(42) Wang, J.; Wolf, R. M.; Caldwell, J. W.; Kollman, P. A.; Case, D. A. *J. Comput. Chem.* **2004**, *25*, 1157−1174.
(43) Bayly, C. I.; Cieplak, P.; Cornell, W.; Kollman, P. A. *J. Chem. Phys.* **1993**, *97*, 10269−10280.
(44) Cieplak, P.; Cornell, W. D.; Bayly, C.; Kollman, P. A. *J. Comput. Chem.* **1995**, *16*, 1357−1377.
(45) Fox, T.; Kollman, P. A. *J. Phys. Chem. B* **1998**, *102*, 8070−8079.
(46) Becke, A. D. *Phys. Rev. A* **1988**, *38*, 3098−3100.
(47) Lee, C.; Yang, W.; Parr, R. G. *Phys. Rev. B: Condens. Matter* **1988**, *37*, 785−789.
(48) Stephens, P. J.; Devlin, F. J.; Chabalowski, C. F.; Frisch, M. J. *J. Phys. Chem.* **1994**, *98*, 11623−11627.
(49) Frisch, M. J.; Trucks, G. W.; Schlegel, H. B.; Scuseria, G. E.; Robb, M. A.; Cheeseman, J. R.; Montgomery, J. A., Jr.; Vreven, T.; Kudin, K. N.; Burant, J. C.; et al. *Gaussian 03, revision E.01*; Gaussian, Inc.: Wallingford, CT, 2004.
(50) Darden, T; York, D; Pedersen, L. *J. Chem. Phys.* **1995**, *103*, 8577−8593.
(51) Hess, B; Bekker, H; Bendersen, H. J. C.; Fraaije, J. G. E. M. *J. Comput. Chem.* **1997**, *18*, 1463−1472.
(52) Hess, B.; Kutzner, C.; Spoel, D. V. D.; Lindahl, E. *J. Chem. Theory Comput.* **2008**, *4*, 435−447.
(53) http://www.gromacs.org/ ( accessed July 7, 2012).
(54) Hornak, V.; Abel, R.; Okur, A.; Strockbine, B.; Roitberg, A.; Simmerling, C. *Proteins* **2006**, *65*, 712−725.
(55) Jensen, M. O.; Park, S.; Tajkhorshi, d. E.; Schulten, K. *Proc. Natl. Acad. Sci. U.S.A.* **2002**, *99*, 6731−6736.
(56) Khurana, E.; Nielsen, S. O.; Ensing, B.; Klein, M. L. *J. Phys. Chem. B* **2006**, *110*, 18965−18972.
(57) Jarzynski, C. *Phys. Rev. Lett.* **1997**, *78*, 2690−2693.
(58) Kumar, S.; Rosenberg, J. M.; Bouzida, D.; Swendsen, R. H.; Kollman, P. A. *J. Comput. Chem.* **1992**, *13*, 1011−1021.
(59) Victor, L. C.; Javier, R.; Javier, M. S. *J. Phys. Chem. B* **2012**, *116*, 469−475.
(60) Fangqiang, Z.; Gerhard, H. *J. Comput. Chem.* **2012**, *33*, 453−465.
(61) Rong, C.; Shin-Ho, C. *Biochemistry* **2012**, *51*, 1976−1982.
(62) Lemkul, J. A.; Bevan, D. R. *J. Phys. Chem. B* **2010**, *114*, 1652−1660.
(63) Hub, J. S.; de Groot, B. L. *Biophys. J.* **2006**, *91*, 842−848.
(64) Patey, G. N.; Valleau, J. P. *Chem. Phys. Lett.* **1973**, *21*, 297−300.
(65) Torrie, G. M.; Valleau, J. P. *Chem. Phys. Lett.* **1974**, *28*, 578−581.
(66) Torrie, G. M.; Valleau, J. P. *J. Comput. Phys.* **1977**, *23*, 187−199.